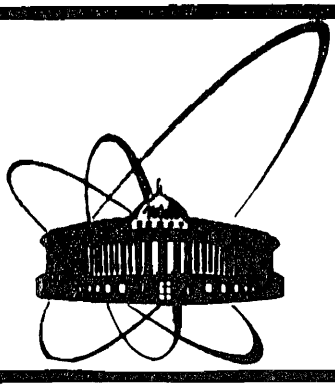

объединенный
институт
ядерных
исследований
дубна

E2-86-707

B.Z.Kopeliovich, B.G.Zakharov*

EFFECTS OF HADRONIC COLOUR STRUCTURE IN QUASI-ELASTIC AND CHARGE EXCHANGE SCATTERING ON NUCLEI

Submitted to "ЯФ"

* Institute of Terrestrial Physics,
Academy of Sciences of the USSR

1986

I. Introduction

One of the most impressive consequences of the QCD is the strong dependence of the hadron interaction cross section upon its size [1-4]. Colourless hadrons can interact with a coloured field only due to spatial distribution of the colour charge inside it. Point-like hadrons do not interact. The interaction cross section tends to zero as r^2 when transverse dimension of the hadron $r \to 0$. A close analogy in QED is the positronium scattering.

This result makes the QCD essentially different from the other models. The Regge phenomenology gives no relation between the hadronic interaction cross section and the radius. In the additive quark model a decrease of the interquark distance leads only to small diminishing of the interaction cross section due to an increase of the Glauber-like screening.

It seems that such considerable distinction of the model predictions can be easily observed experimentally.

It was suggested in papers [5,6] that nuclei should be used as a filter, discriminating transverse size of high energy hadrons. The diffractive scattering and K_s meson regeneration, which are sensitive to the transparency of nuclear matter, are actually well described [5,7]. But a good agreement is also obtained in the additive quark model [8-10].

The smallness of the cross sections of the hadrons containing heavy quarks is connected in QCD with the small size of such hadrons [3,4]. In the additive quark model this is explained by the weakness of the heavy quark interaction. Comparison of the results of calculations in both models demonstrates surprising coincidence for the total hadronic cross sections [11].

The above examples show that the choice of the "smoking gun" experiment is not so easy. This is the subject of the present paper.

One can suggest that a hadron should be scattered on a nucleon target with different values of momentum transfered, in the presence of absorbing nuclear matter. If scattering with larger momentum transfer is dominated by smaller hadronic transverse dimension, then according to QCD prediction one should expect nuclear matter to become more transparent with the transfer momentum increasing. The expected effect

is large: if hadron is absorbed by nuclear matter, then A-dependence of the cross section is about $A^{1/3}$, but if nucleus becomes transparent, then A-dependence is much more steep ~ A.

The quasi-elastic scattering is considered as an example in Sec. 2 of this paper. It is shown that this process disobeys the conditions mentioned above. It follows from the internal colour structure of the Pomeron, which leads to absence of the hadron formfactor in the elastic scattering amplitude. In the double gluon exchange approximation (DGA), for instance, in the case of meson scattering with high momentum transfered, the two gluons can be coupled to different valence quarks of the meson (Fig. 1b). Thus the momentum transfered is divided between two quarks and the meson does not disintegrate even if it has a large transverse dimension. The calcula-

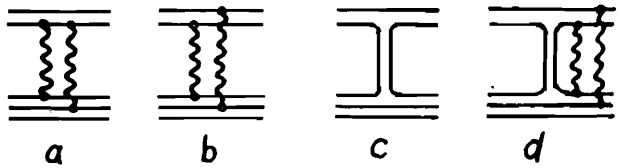

Fig. 1. Different contributions to the meson-nucleon elastic scattering amplitude. Pomeron exchange in DGA (a,b); Reggeon exchange (c); Reggeon-Pomeron cut (d).

tions performed in DGA for different nuclei really demonstrate that the value of $A_{eff} \sim A^{1/3}$ and it weakly depends on q^2 (the momentum transfered squared). It is worth noting that the value of A_{eff} only becomes large $A_{eff} \sim A$ at very large $q^2 \gg (2\alpha'_{I\!P} \ln s/s_0)^{-1}$, where $\alpha'_{I\!P} \approx 0.1$ (GeV/c)$^{-2}$ is the parameter of the Pomeron trajectory slope.

On the contrary, in the case of reactions with the quantum number exchange one can believe that the momentum is only transfered to one of the quarks. This is seen in the quark diagram shown in Fig. 1c, which corresponds to the Reggeon exchange.

In Sec. 3 the charge exchange quasi-free reaction $\pi^{\pm} \to \eta^{0}$ on nuclei is considered. The experimental data show the rapid growth of A_{eff} with q^2 in accordance with theoretical prediction.

More high statistics data are available for the reaction of charge exchange $\pi^{-} \to \pi^{0}$ considered in Sec. 4. The experimental data contradict the Glauber /12/-Sitenko /13/ approximation, but they are in good agreement with the above consideration.

Polarization phenomena in the quasi-elastic scattering on nuclei are considered in Sec. 5. It is shown that the spin-flip amplitude is more enhanced by the nucleus than the nonflip one. As a result, polarization in scattering on a nucleus is considerably larger at high q^2 than that for a nucleon target.

The results of the work are discussed in Sec. 6. Some new experiments sensitive to QCD predictions are also proposed.

2. Quasi-elastic scattering on nuclei

Let us consider the scattering of the $q\bar{q}$-pair with the relative transverse distance $\vec{\tau}$ on the nucleon target. In the DGA shown graphically in Fig. a,b one can calculate the value of the scattering amplitude $f_{el}(q,\tau)$ corresponding to the momentum transfer q.

$$f_{el}(q,\tau) = i\frac{8}{3}\alpha_s^2 \int d^2k \left[\exp\left(\tfrac{i}{2}\vec{q}\vec{\tau}\right) - \exp\left(i\vec{k}\vec{\tau}\right)\right] \times$$
$$\left[\exp\left(-\tfrac{1}{6}\tau_N^2 q^2\right) - \exp\left(-\tfrac{1}{2}\tau_N^2\left(k^2 - \tfrac{1}{4}q^2\right)\right)\right] \times \qquad (1)$$
$$\left[\left(\tfrac{1}{2}\vec{q} - \vec{k}\right)^2 + m_g^2\right]^{-1}\left[\left(\tfrac{1}{2}\vec{q} + \vec{k}\right)^2 + m_g^2\right]^{-1}.$$

Here $\alpha_s = g^2/4\pi$, where g is the QCD coupling constant; τ_N^2 is mean square of the nucleon radius; m_g is the gluon effective mass introduced to take into account the confinement. The value of m_g is of the order of the inverse hadron radius and is chosen to be equal to 0.17 GeV.

The elastic πN -scattering amplitude $f_{el}^{\pi N}(q)$ is a result of averaging of expression (1) over $\vec{\tau}$ with the weight $|\Psi_\pi(\tau)|^2$, where Ψ_π is the pion wave function

$$f_{el}^{\pi N}(q) = \langle f_{el}(q,\tau)\rangle_\tau \equiv \int d^2\tau\, |\Psi_\pi(\tau)|^2 f_{el}(q,\tau). \qquad (2)$$

Though the DGA is obviously oversimplified, it describes the experimental data /3,4/ well.

We have calculated the slope parameter $B(q,\tau) = 2d\ln f(q,\tau)/dq^2$ for scattering of the $q\bar{q}$ pair on a nucleon. We used the Gauss parametrization for the pion wave function and values of parameters $\tau_\rho = 0.7$ fm; $\tau_\pi = 0.59$ fm; $\alpha_s = 0.826$; $\sigma_{tot}^{\pi N} = 24.5$ mb.

Fig. 2 demonstrates the q^2 dependence of the slope parameter $B(q,\tau)$ for different values of τ. It is seen that $B(q,\tau)$ slightly depends on τ in the region $q^2 \gtrsim 0.5$ (GeV/c)^2. This is the result of the dominance of the diagram in Fig. 1b in this region. Its contribution is insensitive to the hadron dimension.

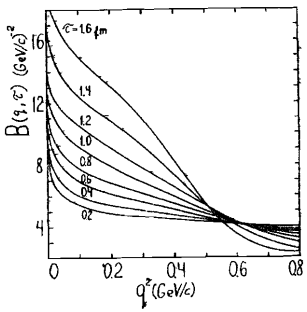

Fig. 2. Dependence of the slope parameter $B(q,\tau)$ upon q^2 for different values of τ.

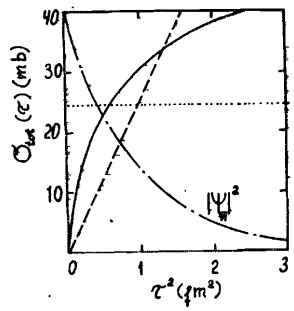

Fig. 3. Total cross section of $q\bar{q}$ pair interaction with a nucleon as a function of τ^2-interquark relative impact parameter squared. The solid curve corresponds to DGA (version I). The dashed curve corresponds to the parametrization (3) (version II).

The τ^2 dependence of the total cross section of the $q\bar{q}$ pair interaction with a nucleon $\sigma_{tot}(\tau) = 2\,\mathrm{Im}\, f_{el}(0,\tau)$ can be determined from (1) and is shown in Fig. 3. At a small interquark distance $\tau \to 0$ the cross section decreases as $\sigma_{tot}(\tau) \propto \tau^2 \ln\tau$. Such behaviour is connected, as was mentioned above, with the dipole character of the interaction, in QCD. The factor $\ln\tau$ is the most model-dependent one. It is the result of using the nonrelativistic quark model and DGA. One can use a simpler form of $\sigma_{tot}(\tau)$

$$\sigma_{tot}(\tau) = \frac{\tau^2}{\langle \tau_\pi^2 \rangle}\, \sigma_{tot}^{\pi N} \qquad (3)$$

which is also shown in Fig. 3.

Now let us consider the reaction of quasi-elastic single scattering on a nucleon inside a nucleus. To calculate inelastic corrections to the Glauber /12/-Sitenko /13/ approximation (GSA), it is convenient to use the eigenstate method /14,9/. If the energy is large enough $E/\mu^2 \gg R_A$, where μ is a massive parameter, the fluctuations of the relativistic hadron transverse dimension τ are "frozen" during passing a nucleus. Thus the hadron-nucleus scattering amplitude is a result of the averaging over τ of the scattering amplitude with the fixed value of τ /5,6/.

The differential cross section of the quasi-elastic single scattering with the momentum transfer q has a form

$$\frac{d\sigma^{(1)}_{Qel}}{dq^2} = \frac{1}{4\pi} \sum_{A',N} \left| \langle A'\pi N | \hat{f}(q) | A\pi \rangle \right|^2 = \sum_{N=p,n,\chi_f} \frac{A_N}{8\pi} \int d^2\tau\, d^2\tau'$$

$$d^3\tau\, d^3\tau' \left|\Psi_\pi(\tau)\right|^2 \left|\Psi_\pi(\tau')\right|^2 \varphi_f^*(\tau)\, \rho_N(\tau,\tau') \exp\left[i\vec{q}\,(\vec{\tau}-\vec{\tau}')\right] \varphi_f(\tau') \quad (4)$$

$$\langle \chi_f | \hat{f}_{el}(\vec{q},\vec{\tau}) \hat{f}^+_{el}(\vec{q},\vec{\tau}') | \chi_f \rangle \exp\left[-\tfrac{1}{2}\sigma_{tot}(\tau) T(b) - \tfrac{1}{2}\sigma_{tot}(\tau') T(b)\right].$$

The following notations are used here: $A_N = Z$ - the number of protons, if $N = p$, $A_N = A-Z$ - the number of neutrons if $N = n$; $\varphi_f(\tau)$ and $|\chi_f\rangle$ are the coordinates of the spin wave functions of the recoil nucleon; $\rho_N(\vec{\tau},\vec{\tau}')$ is the coordinate density matrix of a nucleon inside a nucleus; $\hat{f}_{el}(\vec{q},\vec{\tau})$ is the amplitude of scattering of a $q\bar{q}$ system on a nucleon, which has a form of 2x2 matrix; $T(b) \approx A\int_{-\infty}^{\infty} dz\, \rho(z,\vec{b})$ is the nucleus profile function, where $\rho(\vec{\tau}) = \rho_N(\vec{\tau},\vec{\tau})$ is the nuclear density.

The sum over final states of the nucleus and integration over momentum of the recoil nucleon ($\vec{q}$ is fixed) give $\sum_f \varphi_f^*(\vec{\tau})\varphi_f(\vec{\tau}') = \delta(\vec{\tau}-\vec{\tau}')$. Here we ignore the spin structure of the elastic scattering amplitude $\hat{f}_{el}(\vec{q},\vec{\tau})$ (see below Sec. 4). Then expression (4) is simplified to

$$\frac{d\sigma^{(1)}_{Qel}}{dq^2} = \frac{1}{4\pi} \int d^2b\, T(b) \left| \left\langle f_{el}(\vec{q},\vec{\tau}) \exp\left[-\tfrac{1}{2}\sigma_{tot}(\tau) T(b)\right] \right\rangle_\tau \right|^2. \qquad (5)$$

The result of calculations of the effective atomic number $A_{eff}(q) = \left[d\sigma^{(1)}_{Qel}(\pi A)/dq^2\right] / \left[d\sigma_{el}(\pi N)/dq^2\right]$ by using formulee (5), (1) is shown in Fig. 4 for different nuclei. The nucleus density has been taken in the Woods-Saxon form /15/. It is seen that $A_{eff}(q^2)$ slightly depends on q^2. As was explained in the Introduction, this is related to colour structure of the Pomeron.

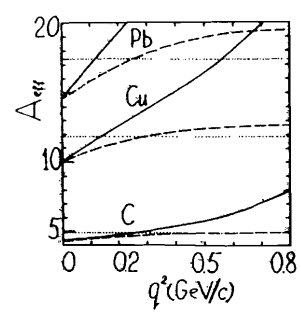

Fig. 4. q^2-dependence of A_{eff} for quasi-elastic single scattering calculated in DGA for different nuclei (solid curves). The dashed curves are the same, but including the multiple scattering contribution. The dotted line corresponds to the GSA.

Fig. 4 also shows the results of the calculation in the framework of the GSA. The value of A_{eff} is independent of q^2 in this approximation. It is interesting that at small q^2 the cross section given by formula (5) is below the result of the GSA. In other words, the inelastic corrections in this case do not make the nucleus medium transparent but obscure. This is the result of integration over τ in (5) where the factor $f(q,\tau)$ is large at high values of τ but the exponential factor is large only at small values of τ.

It should be noted that at sufficiently large values of q^2 the relativistic wave function of the hadron should be used. Hadronic configurations of large dimension with smeared gluonic cloud are suppressed in the elastic scattering with high q^2. Consequently, one can expect considerable growth of $A_{eff}(q^2)$ /16/. Corresponding values of q^2 are determined by the dimension of a gluonic cloud $q^2 \gg (2\alpha'_{I\!P} \ln s)^{-1}$, where $\alpha'_{I\!P} \approx 0.1$ (GeV/c)$^{-2}$ is the slope parameter of the Pomeron trajectory, s is the energy squared in c.m.s. in GeV^2. There are no data for this region. Measurements of the recoil nucleon and reconstruction of quasi-elastic kinematics are necessary to avoid multiple rescattering contributions to $A_{eff}(q^2)$. Otherwise the latter may be calculated. The double scattering contribution has a form

$$\frac{d\sigma^{(2)}_{qel}}{dq^2} = \frac{1}{8\pi}\int d^2b\, T^2(b) \int \frac{d^2k}{(2\pi)^2} \Big| \Big\langle f_{qel}(\vec{k},\vec{\tau}) f_{qel}(\vec{q}-\vec{k},\vec{\tau}) \times \exp\Big[-\tfrac{1}{2}\sigma_{tot}(\tau)T(b)\Big]\Big\rangle_{\tau}\Big|^2 . \qquad (6)$$

Since the inelastic corrections to the single scattering contribution has been found to be small and the momentum transfer in the double scattering is on the average divided fifty-fifty, expression (6) can be estimated in the GSA at medium values of $q^2 \lesssim 1$ (GeV/c)^2. The triple and higher rescattering contributions turn to be negligibly small in this region. The results of calculation of the quasi-elastic cross section including (6) are shown in Fig. 4.

3. Charge exchange reaction $\pi^{\pm}A \to \eta^{\circ} X$

Strong q^2-dependence of A_{eff} can be expected in charge exchange reactions. As was considered in the Introduction, this is due to hadronic formfactor in the charge exchange amplitude (see Fig. 1c) which picks out compressed quark configurations in scattered hadron at high values of $q^2 \gtrsim \langle\tau^2\rangle^{-1}$.

Let us at first consider the reaction $\pi^- p \to \eta^{\circ} n$ which is convenient because of the pole (A_2) dominance /17,18/ up to the values of $q^2 \approx 1$ (GeV/c)^2. The single-scattering contribution to the cross section of quasi-free charge exchange scattering $\pi^- A \to \eta^{\circ} X$ has the

form

$$\frac{d\sigma^{(1)}(\pi^- A \to \eta^{\circ} X)}{dq^2} = \frac{1}{8\pi}\frac{Z}{A}\int d^2b\, T(b)\, Sp\Big\{\Big\langle \hat{f}^{+}_{cex}(\vec{q},\vec{\tau}) \times \exp\Big[-\tfrac{1}{2}\sigma_{tot}(\tau)T(b)\Big]\Big\rangle_{\tau}\Big\langle \hat{f}_{cex}(\vec{q},\vec{\tau}) \exp\Big[-\tfrac{1}{2}\sigma_{tot}(\tau)T(b)\Big]\Big\rangle_{\tau}\Big\}. \qquad (7)$$

The averaging over τ is taken here with the weight factor $\Psi^*_{\eta}(\tau)\,\Psi_{\pi}(\tau)$. We assume further that the coordinate parts of the wave functions $\Psi_{\eta}(\tau)$ and $\Psi_{\pi}(\tau)$ coinside (according to SU_3) and, consequently, $\sigma_{tot}(\eta N)$ and $\sigma_{tot}(\pi N)$ are equal.

The amplitude $\hat{f}_{cex}(\vec{q},\vec{\tau})$ is a 2x2 matrix in the nucleon spin space. It can be written down as follows

$$\hat{f}_{cex}(\vec{q},\vec{\tau}) = C\,[A(\vec{q},\vec{\tau}) + i q(\vec{\sigma}\vec{n})\,B(\vec{q},\vec{\tau})]. \qquad (8)$$

Here the constant C includes all factors independent of $\vec{q}$ and $\vec{\tau}$; $\vec{n}$ is the unity vector which is normal to the scattering plane; $\vec{\sigma}$ are the Pauli matrices. The spin amplitudes can be written down in the form

$$A(\vec{q},\vec{\tau}) = \exp\left(\tfrac{i}{2}\vec{q}\vec{\tau} - \lambda q^2\right)$$
$$B(\vec{q},\vec{\tau}) = \beta\, A(\vec{q},\vec{\tau}). \qquad (9)$$

The experimental data /17,18/ at 40 GeV are well described with the values of $\beta = 6.1\ GeV^{-1}$, $\lambda = 3.4$ (GeV/c)$^{-2}$.

Calculations of $Z^{(1)}_{eff}(q^2) = \frac{d\sigma^{(1)}(\pi^- A \to \eta^{\circ} X)}{dq^2} \Big/ \frac{d\sigma(\pi^- p \to \eta^{\circ} n)}{dq^2}$ have been performed by using formula (8) with the following alternative for $\sigma_{tot}(\tau)$ dependence: variant I corresponds to the DGA and expression (1); variant II corresponds to simple form (3). Results are shown in Fig. 5. It is seen that q^2-dependence of Z_{eff} is much stronger than

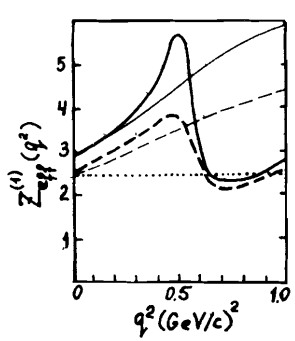

Fig. 5. $Z^{(1)}_{eff}(q^2)$ for quasi-free charge exchange single scattering on the ^{12}C nucleus. The solid and dashed curves correspond to the versions II and I respectively. The thin curves correspond to the charge exchange $\pi^- \to \eta^{\circ}$ and to the reaction $\pi^- \to \pi^{\circ}$ in the case of pure pole contribution. The thick curves are the predictions for the latter reaction if the pole-cut interference is taken into account (see the text). The dotted line shows the GSA result.

in quasi-elastic scattering, as was expected. Comparison with results of GSA also shown in Fig. 5 at small q^2 demonstrates that inelastic corrections to the charge exchange scattering make the nuclear medium more transparent which is not the case with the quasi-elastic scattering.

Double scattering contribution to the cross section (single charge exchange and single elastic scattering) has the form

$$\frac{d\sigma^{(2)}(\pi^- A \to \eta^0 X)}{dq^2} = \frac{1}{8\pi}\,\frac{Z(A-1)}{A^2}\int d^2b\; T^2(b)\int\frac{d^2k}{(2\pi)^2}\; Sp\Big\{\Big\langle \hat{f}^{+}_{cex}(\vec{k},\vec{\tau}) \times$$

$$f^{*}_{el}(\vec{q}-\vec{k},\vec{\tau})\exp\Big[-\tfrac{1}{2}\sigma(\tau)T(b)\Big]\Big\rangle_{\tau} \times \qquad (10)$$

$$\Big\langle \hat{f}_{cex}(\vec{k},\vec{\tau}) f_{el}(\vec{q}-\vec{k},\vec{\tau})\exp\Big[-\tfrac{1}{2}\sigma(\tau)T(b)\Big]\Big\rangle_{\tau}\Big\}.$$

As in the case of quasi-elastic scattering, correction (10) can be estimated in the GSA and higher order rescattering corrections can be neglected.

The results of calculation made with formulae (7)-(10) for nucleus ^{12}C in two variances are compared in Fig. 6 with the experimental data /18/ at 40 GeV. The GSA curve is also presented. It is seen that the accuracy of the data is insufficient to prefer any of the theoretical curves.

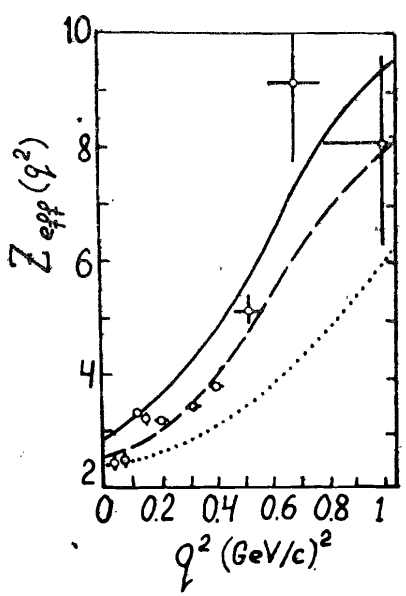

It is worth noting that formulae (7)-(10) are also valid for the reaction $\pi^+ A \to \eta^0 X$ but with exchange $Z \rightleftarrows A - Z$. Corresponding predictions for the ratio of cross section $R_{A/Be} = \frac{d\sigma(\pi^+ A \to \eta^0 X)/dq^2}{d\sigma(\pi^+ Be \to \eta^0 X)/dq^2}$ for ^{64}Cu and ^{208}Pb nuclei are shown in Fig. 7 in versions I, II and the GSA.

Fig. 6. $Z_{eff}(q^2)$ for the charge exchange scattering $\pi^- A \to \eta^0 X$ on the ^{12}C nucleus. Experimental points are from Ref. /18/. Calculations are made with multiple scattering corrections included in version II (solid curve), in the version I (dashed curve) and in the GSA (the dotted curve).

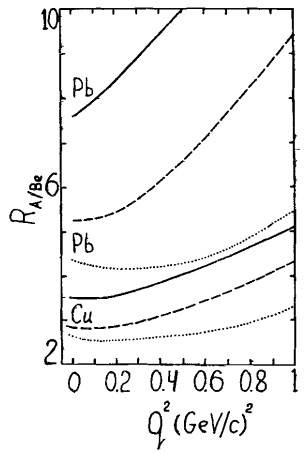

Fig. 7. Predictions for $R_{A/Be}(q^2) = \frac{d\sigma(\pi^+ A \to \eta^0 X)/dq^2}{d\sigma(\pi^+ Be \to \eta^0 X)/dq^2}$ for Pb and Cu nuclei. The solid, dashed and dotted curves correspond to versions II, I and the GSA respectively.

4. Charge exchange reaction $\pi^- A \to \pi^0 X$

Similar calculations for the reaction $\pi A \to \pi^0 X$ may have some specific difference due to characteristic dip structure /17,18/ in the q^2-dependence of the cross section of the reaction $\pi^- p \to \pi^0 n$ at $q^2 \approx 0.6$ (GeV/c)^2. One of the popular interpretations /19/ of this dip is zero value of the ρ-pole residue in the wrong signature nonsense point $q^2 \approx 0.6$ (GeV/c)^2 due to ρ-f exchange degeneracy. In this case the differential cross section of charge exchange single scattering on a nucleus has a dip in the same point as on the hydrogen target. Results of calculation in versions I, II are close to that for $\pi^- A \to \eta^0 X$ and are shown in Fig. 5.

Another possibility /19/ of the dip appearance is destructive interference of the ρ pole and ρ-$I\!P$ cut contributions (see Fig. 1 c,d). This version naturally explains the difference in the positions of zeros in spin-flip and nonflip (cross-over point) amplitudes. It is clear that the ratio of ρ pole and $\rho I\!P$-cut contributions for a nucleus differs from that for a hydrogen target. Indeed, at large values of q^2 the ρ-pole exchange picks out hadronic fluctuations of small dimension according to the above consideration. The nucleus becomes transparent and the ρ-pole contribution is enhanced by a factor of $\sim Z$. On the contrary the $\rho I\!P$-cut contribution (Fig. 1d) is similar to the elastic scattering (Fig. 1b). It does not pick out small configurations in a hadron and is enhanced on a nucleus only by a factor of $\sim Z^{1/3}$. Such change of relation between pole and cut leads to displacement of the dip position to higher values of q^2, where it can be filled by a non-flip amplitude contribution.

A single scattering contribution to the differential cross section in this case is calculated by using formula (7) but the form of spin amplitudes differs from (9).

$$A(q,\tau) = \exp\left(\tfrac{i}{2}\vec{q}\vec{\tau} - \lambda q^2\right) - \frac{\gamma}{2a}\exp\left(-\tfrac{1}{2}aq^2 - \frac{\tau^2}{8a}\right)$$

$$B(q,\tau) = \beta\exp\left(\tfrac{i}{2}\vec{q}\vec{\tau} - \lambda q^2\right) - \frac{\beta\gamma}{4a}\exp\left(-\tfrac{1}{2}aq^2 - \frac{\tau^2}{8a}\right). \qquad (11)$$

The terms with the factor γ are the $\rho\mathbb{P}$-cut contribution. They have been calculated under an assumption that slopes of the Pomeron and ρ-pole exchange amplitudes are the same and equal to a/2. Parameters β and λ differ from that in $\pi\to\gamma$ reaction. They are found by fitting the experimental data [17,18]: $\gamma = 5.95$, $|\beta| = 3.7\ GeV^{-1}$, $\lambda = 4.5\ GeV^{-2}$, $a = 6\ GeV^{-2}$.

Results of calculation of the single scattering contribution to the effective number $Z_{eff}^{(1)}$ are shown in Fig. 5 for versions I and II. The bump-dip structure of curves is due to different positions of minima in cross sections on a nucleus and hydrogen. It is seen that the two theoretical treatments of the dip structure in the $\pi^-p\to\pi^0 n$ differential cross section discussed above give quite different predictions for $Z^{(1)}(q^2)$. Thus investigation of hadron-nucleus interactions can help to solve the problem of the dip interpretation which is till open.

Unfortunately, the available data [18] are obtained in inclusive measurements. So one should include the multiple scattering corrections. The double scattering contribution can be calculated using expression (10), where $\hat{f}_{cex}$ is given by (8), (11). Besides one should take into account the fact that only the events without charged recoil particles were permitted in experiment. Thus expression (10) should be multiplied by (A-Z)/(A-1).

Results of calculation of Z_{eff} are compared with the data [18] in Fig. 8. The best agreement is for the curve calculated in version II, which corresponds to maximal transparency of a nucleus. It is also seen that the data prefer the model connecting origin of the dip in the $\pi^-p\to\pi^0 n$ reaction with the cut. The GSA stongly contradicts the data. Some disagreement at very small q^2 seen in Fig. 8 is a result of the Fermi-statistics being disregarded.

Note in conclusion that one should not pick out version I or II on the ground of the quality of description of the data in Fig. 8. Calculating the inelastic corrections, we ignored the triple Pomeron contribution.

5. Polarization effects

Elastic scattering polarization at high energies is the result of interference of the nonflip amplitude f_{++} dominated by the Pomeron

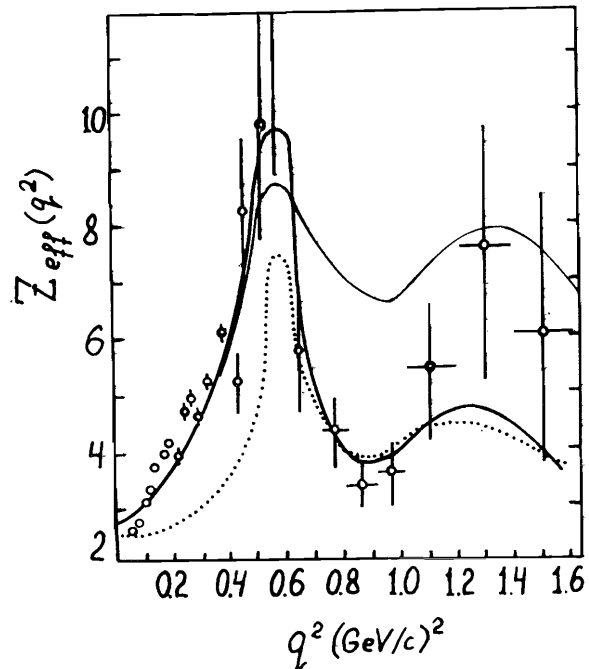

Fig. 8. The same as in Fig. 6 for the reaction $\pi^-A\to\pi^0X$ on the ^{12}C nucleus. The thick and thin solid curves are calculated in version II. They differ from each other in the same way as the corresponding curves in Fig. 6.

and spin-flip amplitude f_{+-} dominated by the Reggeons (ρ, A_2). The latter decreases with the energy, so polarization is small at high energies.

It follows from the above consideration that Pomeron and Reggeon exchange amplitudes are enhanced in quasi-free scattering on nuclei in a different way. The former slightly depends on q^2 and is weekly enhanced by $\sim A^{1/3}$. The latter steeply grows with q^2 and is enhanced by up to $\sim A$. Thus relation between spin amplitudes is changed on nucleus in favour of f_{+-}. This should result in the growth of polarization.

Polarization of recoil protons in the quasi-elastic isingle scattering $\pi^-A\to\pi^-pX$ is given by the following expression

$$P_0(q^2)\frac{d\sigma^{(1)}_{Qel}}{dq^2} = \frac{Z}{8\pi A}\int d^2b\, T(b) S_p\Big\{(\vec{\sigma}\vec{n})\Big\langle \hat{f}^{+}_{el}(\vec{q},\vec{\tau}) \times \exp\Big[-\tfrac{1}{2}\sigma_{tot}(\tau)T(b)\Big]\Big\rangle_{\tau}\Big\langle \hat{f}_{el}(\vec{q},\vec{\tau})\exp\Big[-\tfrac{1}{2}\sigma_{tot}(\tau)T(b)\Big]\Big\rangle_{\tau}\Big\}. \quad (12)$$

The cross section $d\sigma_{Qel}/dq^2$ is given by expression (5); $\hat{f}_{el}(\vec{q},\vec{\tau}) = \hat{f}^{I\!P}_{el}(\vec{q},\vec{\tau}) + \hat{f}^{R}_{el}(\vec{q},\vec{\tau})$ is the sum of the Pomeron and Reggeon contributions; the amplitudes $\hat{f}^{I\!P,R}_{el}$ have the form of (8). We put $B^{I\!P}(\vec{q},\vec{\tau}) = 0$ and took $B^{\rho}(\vec{q},\vec{\tau})$ in the form of (11), i.e. included the cut contribution. The result of calculation of the ratio of polarizations in the quasi-elastic single scattering on Pb and in the elastic πN scattering as a function of q^2 is shown in Fig. 9. It is seen that in the region $q^2 \approx 1$ (GeV/c)^2 the enhancement factor exceeds two.

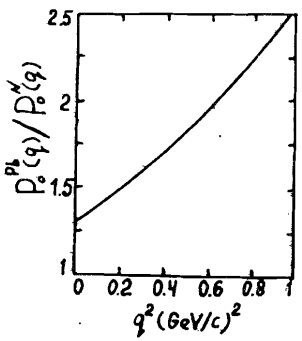

Fig. 9. Ratio of polarizations in the quasi-elastic scattering on Pb and hydrogen targets, calculated in version II.

We considered polarization of the recoil nucleons. An effect of the same order is expected for scattered protons in the quasi-elastic proton-nucleus scattering. It should be emphasized that registration of the recoil nucleon is needed in any case to execute the quasi-elastic single scattering kinematics. Additional rescatterings suppress polarization . On the other hand in the charge exchange single scattering polarization should be suppressed at large q^2. In fact polarization in this case is due to $\rho I\!P$-cut and ρ-pole interference. The former, as was considered above, has little nuclear enhancement. But if polarization is due to interference of different poles (ρ, ρ'), then polarization in a nuclear reaction is the same as on hydrogen. Thus precise measurements of polarization in the quasi-free charge exchange single scattering can yield useful information about the origin of the charge exchange scattering polarization.

6. Discussion

Here we proposed an effective method to verify the QCD prediction about strong dependence of hadronic cross sections in their size. It is shown that in the quasi-free charge exchange scattering on a nucleus at medium values of $q^2 \lesssim 1$ (GeV/c)^2 nuclear matter is transparent for the scattered hadron, because its transverse dimension is small. The phenomenon is observed experimentally and this is the first essential justification of smallness of point-like hadron interaction.

Nevertheless new data obtained in special experiments are needed.

1. It is desirable to have some data on the cross section of quasi-free charge exchange single scattering. Kinematics corresponding to the binary reaction should be controlled experimentally. Data obtained on nuclei heavier than ^{12}C are also necessary.

2. It is interesting to measure quasi-elastic single scattering at large momentum transfer, at least several GeV/c.

3. Measurement of the polarization effects is possible with polarized nuclear targets, or by means of analysis of the recoil nucleon polarization. Another possibility is measurement of asymmetry in polarized proton beam scattering.

4. A possible interesting experiment of this type is coherent production of a symmetrical pair of particles with large p_T (relative transverse momentum) on nuclei. This process might have an observable cross section at sufficiently high energies. A large p_T corresponds to a small interquark distance inside the incident hadron. Thus nuclear matter should be transparent and this should be displayed in A-dependence.

During performing this work we were essentially supported by helpful discussions with L.I.Lapidus. We are indepted also to V.V. Anisovich and M.I.Strikman for useful comments.

References

1. Low F., Phys.Rev., 1975, D12, p. 163
2. Nussinov S., Phys.Rev.Lett., 1975, 34, p. 1286
3. Gunion J.F., Soper H., Phys.Rev., 1977, D15, p. 2617
4. Levin E.M., Ryskin M.G. Yad.Fiz., 1981, 34, p. 1114
5. Zamolodchikov A.B., Kopeliovich B.Z., Lapidus L.I., JETP Lett., 1981, 33, p. 612
6. Bertch J., Brodsky S.J., Goldhaber A.S., Gunion J.G., Phys.Rev. Lett., 1981, 47, p. 267
7. Zamolodchikov A.B., Kopeliovich B.Z., Lapidus L.I., Yad.Fiz., 1982, 35, p. 129
8. Kopeliovich B.Z., Nikolaev N.N. Z.Phys.C, 1980, 5, p. 333
9. Kopeliovich B.Z., Lapidus L.I., JETP Lett., 1978, 28, p. 664
10. Kopeliovich B.Z., Lapidus L.I., Vegh L., Yad.Fiz., 1982, 35, p.1514
11. Pak A.S., Sadykov N.O., Tarasov A.V., Yad.Fiz., 1985, 42, p.975
12. Glauber R.J., High energy collision theory, Lectures in theoretical physics, v. 1, ed. W.E.Britten and L.G.Dunham, Interscience N.Y., 1959

13. Sitenko O.G., Ukrainian Physical Journal, 1959, 4, p. 152
14. Kopeliovich B.Z., Lapidus L.I. In: Proc.of the 5th Int.Sem.on High Energy Physics Problems, JINR, D1,2-12036, Dubna, 1978, p. 469
15. De Yaeger C.W., De Vries H., De Vries C., Atomic Data and Nuclear Data Tables, 1974, 14, p. 479
16. Mueller A.H., Columbia University preprint, CU-TP-232, 1982
17. Apel V.D. et al., Nucl.Phys., 1979, B152, p. 1; ibid. 1979, 154B, p. 189
18. Apokin B.D. et al., Yad.Fiz., 1982, 36, p. 1191
19. Collins P.D.B. An Introduction to Regge Theory and High Energy Physics, Moscow, Atomizdat, 1980

Received by Publishing Department
on October 24, 1986.

SUBJECT CATEGORIES OF THE JINR PUBLICATIONS

Index	Subject
1.	High energy experimental physics
2.	High energy theoretical physics
3.	Low energy experimental physics
4.	Low energy theoretical physics
5.	Mathematics
6.	Nuclear spectroscopy and radiochemistry
7.	Heavy ion physics
8.	Cryogenics
9.	Accelerators
10.	Automatization of data processing
11.	Computing mathematics and technique
12.	Chemistry
13.	Experimental techniques and methods
14.	Solid state physics. Liquids
15.	Experimental physics of nuclear reactions at low energies
16.	Health physics. Shieldings
17.	Theory of condenced matter
18.	Applied researches
19.	Biophysics

Копелиович Б.З., Захаров Б.Г.

E2-86-707

Цветовая структура адронов в квазиупругом рассеянии и перезарядке на ядрах

Рассмотрены эффекты экранирования цвета внутри адронов при взаимодействии их с ядрами. Показано, что в реакциях квазисвободной перезарядки на ядрах с ростом переданного импульса ядерная среда должна стать прозрачной для рассеиваемого адрона. Существующие экспериментальные данные подтверждают это предсказание КХД.

Работа выполнена в Лаборатории ядерных проблем ОИЯИ.

Препринт Объединенного института ядерных исследований. Дубна 1986

Kopeliovich B.Z., Zakharov B.G.

E2-86-707

Effects of Hadronic Colour Structure in Quasi-Elastic and Charge Exchange Scattering on Nuclei

Effects of hadronic hidden colour screening are considered in hadron-nucleus interaction. It is shown that in the quasi-free charge exchange reaction nuclear matter becomes transparent for the scattered hadron if the momentum transfer is large enough. The available experimental data confirm this prediction of QCD.

The investigation has been performed at the Laboratory of Nuclear Problems, JINR.

Preprint of the Joint Institute for Nuclear Research. Dubna 1986